arXiv:1610.02450v1 [cond-mat.mtrl-sci] 7 Oct 2016

Fe_3O_4 thin films: controlling and manipulating an elusive quantum material

X. H. Liu, C. F. Chang, A. D. Rata†, A. C. Komarek, and L. H. Tjeng
Max Planck Institute for Chemical Physics of Solids,
Nöthnitzerstr. 40, 01187 Dresden, Germany

†current address: Institute of Physics, Martin Luther University,
Halle-Wittenberg, 06099 Halle, Germany

07 July, 2016

Fe_3O_4 (magnetite) is one of the most elusive quantum materials and at the same time one of the most studied transition metal oxide materials for thin film applications. The theoretically expected half-metallic behavior generates high expectations that it can be used in spintronic devices. Yet, despite the tremendous amount of work devoted to preparing thin films, the enigmatic first order metal-insulator transition and the hall mark of magnetite known as the Verwey transition, is in thin films extremely broad and occurs at substantially lower temperatures as compared to that in high quality bulk single crystals. Here we have succeeded in finding and making a particular class of substrates that allows the growth of magnetite thin films with the Verwey transition as sharp as in the bulk. Moreover, we are now able to tune the transition temperature and, using tensile strain, increase it to substantially higher values than in the bulk.

Keywords: magnetite, thin film, spintronics, Verwey transition, strain, domain

While thousands of studies have been devoted to try to understand the first order Verwey transition in magnetite, the high Curie temperature ($T_C \sim 860$ K) and the half-metallic character of Fe_3O_4 as predicted by band theory [1, 2] have triggered considerable research efforts world wide to make this material suitable for spintronic applications in the form of thin film devices [3, 4, 5, 6, 7]. Using a variety of deposition methods, epitaxial growth on a number of substrates has been achieved [5, 6, 7, 8]. Yet, it is remarkable that in the twenty years of research on Fe_3O_4 thin films, the first order Verwey transition [9] in thin films is always broad [6, 7, 10, 11, 12, 13]. While in the bulk the transition takes place well within 1 K, the reported resistivity curves for the thin films showed transition widths of about 10 K or more. The Verwey transition temperature T_V in thin films is also much lower, with reported values ranging from 100 to 120 K [6, 7, 10, 11, 12, 13] while the stoichiometric bulk has T_V of 124 K.

It has been reported that several factors can affect negatively the Verwey transition in bulk magnetite, such as oxygen off-stoichiometry [14] and cation substitution [15]. The T_V gradually decreases and the transition is claimed to change from a first order to a second or even higher order with increasing oxygen off-stoichiometry or cation substitution. Recently, we have carried out a systematic study on the influence of oxygen stoichiometry for the properties of magnetite thin films [16], and we found that even for the optimal oxygen composition the transition remains broad. In that study, we also discovered that the microstructure of the films play an important role. In particular, with the films having a distribution of domain sizes, a larger spread of the distribution results in a broader transition and a small domain size gives lower transition temperatures. The transition itself is still first order since it shows hysteresis, and there are indications that each domain has its own transition temperature [16]. Various substrates have been used in the literature to grow epitaxial Fe_3O_4 thin films, e.g. MgO, $MgAl_2O_4$, Al_2O_3, $SrTiO_3$, and $BaTiO_3$ [6, 7, 10, 11, 12, 13, 16]. These studies may suggest that the larger the lattice mismatch, the broader the transition and the lower the average transition temperature [16].

Here we have succeeded in finding and making a particular class of substrates that allows

the growth of magnetite thin films with the Verwey transition as sharp as in the bulk. The key principle is to obtain thin films with sufficiently large domains and small domain size distribution. Moreover, using tensile strain we now are able to increase the transition temperature to considerably higher values than that of the bulk. The occurrence of the Verwey transition in the highly anisotropic strained films raises a new question to the intricacies of the interplay between the charge and orbital degrees of freedom of the Fe ions in magnetite, adding another aspect of the elusiveness of this quantum material.

Results

In our quest for substrates that allow for the growth of Fe_3O_4 thin films with large domains and a narrow distribution of domain sizes, we aim first of all for substrates with a very small lattice mismatch. Although MgO is ideal in this respect, the occurrence of anti-phase boundaries [11], which cannot be avoided when growing a (inverse) spinel film on a rocksalt substrate, has a negative effect on the distribution and size of the domains [16]. We therefore restrict ourselves to substrates with the spinel structure. We have identified Co_2TiO_4 with a lattice mismatch of +0.66% as a potential candidate, and managed to prepare large single crystals of this compound using a mirror furnace. Substrates with ≈ 6 mm $\times$ 6 mm epi-polished surfaces have been made out of these crystals. We have also prepared crystals and substrates with somewhat larger lattice mismatch, up to +1.11 %, by partial substitution of the Co with Mn and/or Fe: $Co_{1.75}Mn_{0.25}TiO_4$ and $Co_{1.25}Fe_{0.5}Mn_{0.25}TiO_4$. Details about the preparation and properties of the substrate single crystals are given in the Supplementary Information (Figures S1, S2, and S3)

Figures 1 a-d display the reflection high energy electron diffraction (RHEED) patterns of the clean MgO (001), Co_2TiO_4 (001), $Co_{1.75}Mn_{0.25}TiO_4$ (001), and $Co_{1.25}Fe_{0.5}Mn_{0.25}TiO_4$ (001) substrates, respectively. Figures 1 e-h show the RHEED patterns and Figures 1 i-l present the low energy electron diffraction (LEED) of the 40 nm thick Fe_3O_4 films grown on these respective substrates. Details of the substrate cleaning procedure as well as of the growth conditions

by using the molecular beam epitaxy (MBE) technique can be found in the Methods. The sharpness of the RHEED stripes and the presence of Kikuchi lines, as well the high contrast and sharpness of the LEED spots indicate a flat and well ordered single crystalline (001) surface structure of the films. The presence of the $(\sqrt{2} \times \sqrt{2})$R45° surface reconstruction pattern both in the RHEED and LEED images provides another indication for the high structural quality of the films. The valence states of the Fe ions were investigated by Fe $2p$ core level and valence band x-ray photoelectron spectroscopy (XPS), thereby showing the typical signatures of stoichiometric magnetite, see Fig. S4 in the Supplementary Information. We note that the XPS spectra of the films grown on different substrates are identical, meaning that the substrate has no influence on the chemical composition of the films.

Figure 2a shows the temperature dependence of the resistivity of 40 nm-thick Fe_3O_4 films grown on MgO (001), Co_2TiO_4 (001), $Co_{1.75}Mn_{0.25}TiO_4$ (001), and $Co_{1.25}Fe_{0.5}Mn_{0.25}TiO_4$ (001), as well that of a bulk single crystal Fe_3O_4. We can clearly see that the bulk sample has a sharp Verwey transition at 124 K while the film on MgO shows the typical broad transition at lower temperatures. In contrast, the thin films grown on the spinel substrates all show a very sharp transition, almost as sharp as the bulk. The hysteresis is all within 0.7 K. Most exciting is that now the transition temperatures of these thin films are even higher than that of the bulk. Defining T_{V+} (T_{V-}) as the temperature of the maximum slope of the ρ (T) curve for the warming up (cooling down) branch, the T_{V+} is 127 K for the film grown on Co_2TiO_4 (001) (lattice mismatch +0.66%), 133 K for the film on $Co_{1.75}Mn_{0.25}TiO_4$ (001) (+0.98%), and even 136 K for the film on $Co_{1.25}Fe_{0.5}Mn_{0.25}TiO_4$ (001) (+1.11%), which is 12 K higher than the T_{V+} of the bulk and about 15-35 K higher than the T_{V+} of films of similar thickness reported in the literature so far [6, 7, 10, 11, 12, 13, 16].

Figure 2b plots T_{V+} as a function of the film thickness on the three variants of the spinel substrates, as well that on the rocksalt MgO. The black horizontal line represents the T_{V+} of the bulk single crystal. We can observe that T_{V+} gradually increases with the film thickness, and again, that it is larger for the spinel substrates with the larger lattice constant mismatch between

the film and the substrate. While films with thicknesses of 5 nm and less do not show a Verwey transition, we can clearly see a well defined transition for films when they are 10 nm or thicker. In fact we would like to note that films as thin as 10 nm grown on $Co_{1.75}Mn_{0.25}TiO_4$ (001) (+0.98%) and $Co_{1.25}Fe_{0.5}Mn_{0.25}TiO_4$ (001) (+1.11%) have a T_{V+} which is already comparable to that of the bulk, a highly remarkable result in view of the generally low values even for thicker films known in the literature [6, 7, 10, 11, 12, 13, 16].

We now investigate the strain state of the Fe_3O_4 films grown on the spinel substrates using x-ray diffraction (XRD). Figure 3 presents the reciprocal space mapping of the (115) reflection from a 200 nm-thick film grown on Co_2TiO_4 (001) (+0.66%) (panel a), and from a 80 nm-thick film grown on $Co_{1.25}Fe_{0.5}Mn_{0.25}TiO_4$ (001) (+1.11%) (panel b). The well aligned longitudinally (115) reflection of the film and the substrate demonstrates that the films are fully strained. Long range θ - 2θ XRD data indicate that there are no other phases than Fe_3O_4. We summarize the lattice constants of three variants of the spinel substrates, together with those of the 40 nm, 80 nm and 200 nm Fe_3O_4 films grown on top of these substrates in table 1 from the XRD measurements. As the lattice constant **a** of the substrates increases, i.e. 8.4528 Å, 8.4797 Å, and 8.4898 Å, the lattice constant **c** of the films gradually decreases, e.g. 8.3332 Å, 8.3042 Å, 8.2800 Å, respectively, for the 40 nm films. To compare, the lattice constant of bulk Fe_3O_4 is 8.396 Å. From this we calculate that the Poission ratio is in the range of 0.36-0.38, and that the volume increases as 595.29, 597.20, and 597.19 $Å^3$, respectively, while the volume of bulk Fe_3O_4 is about 591.86 $Å^3$.

We can also get an insight about the microstructure of the films by analyzing the peak profile of the rocking curves of the (115) reflection. From the inverse of the peak width, we can estimate that the average domain size is about 46 nm, 61 nm, and 68 nm for the 40 nm film grown on the three spinel substrates, respectively. These numbers are higher than the 30 nm value found for an equivalent thick film grown on MgO [16], suggesting that the spinel structure of the substrate indeed does help to obtain films of structurally better quality. These results therefore support our conjecture that one needs films with sufficiently large domains and

sufficiently narrow distribution of domain sizes in order to obtain sharp first order transitions. Perhaps this is the solution to remedy the broad first order transitions observed in, for example, V_2O_3 thin films [17, 18, 19], and $RENiO_3$ (RE = Pr, Nd, Sm) thin films [17, 20, 21, 22, 23], e.g. one has to carefully design substrates with a matching lattice structure and sufficiently small lattice mismatch.

Discussion

Having achieved magnetite thin films with a Verwey transition as sharp as the bulk, we now are ready to meaningfully measure and analyze the effect of the strain exerted by the substrate on the transition of the film. It has been reported that the Verwey transition of bulk magnetite becomes broad and that T_V drops linearly with increasing applied hydrostatic pressure and corresponding decrease of the unit cell volume [24, 25, 26, 27]. While the application of negative hydrostatic pressures is experimentally out of reach, our finding that the T_V of the Fe_3O_4 thin films increases when epitaxially grown with increasing unit cell volume indicates that we have in fact succeeded to exert effectively negative pressures on magnetite by using the tensile strain imposed by the carefully chosen spinel substrates. Viewing the Verwey transition as a transition from a Wigner crystal to a Wigner glass of small polarons [28], one can readily accept that changing the one-electron band width, and therefore also the polaron band width, will alter the transition temperature [29]. In particular, enlarging the lattice constant and inter-atomic distances will facilitate the formation of an ordered state in which the different lattice sites have different local valence and orbital states.

Yet it is important to note that the negative pressures exerted on these thin films are by no means isotropic and therefore cannot be considered as being the equivalent of negative hydrostatic pressures. On the contrary, the films are expanded in the plane but compressed along the c-axis direction. This makes the Verwey transition in the tensile strained films even more interesting: would the charge and orbital order be of the same type as in the bulk, for which there

is a lot of debate, see Refs. [30], [31], [32], and references therein. In this respect, we would like to note that the resistivity across the Verwey transition changes by about a factor 10 in the films while it is by a factor 100 in the bulk. Clearly the presence of the substrate limits a full opening of the conductivity gap by putting constraints on the crystal structure. Nevertheless the transition does take place and so the question arises what are the minimal conditions required in terms of the local electronic structure such as the orbital state for such a transition to occur. It would be extremely interesting to address this question by, for example, carrying out charge and/or orbital sensitive resonant x-ray diffraction experiments, see Ref. [32] and references therein.

Methods

Fe_3O_4 thin films were grown by using molecular beam epitaxy (MBE) in an ultra-high vacuum (UHV) chamber with a base pressure in the high 10^{-11} mbar range. High purity Fe metal was evaporated from a LUXEL Radak effusion cell at temperatures of about 1250 $^{\circ}\mathrm{C}$ in a pure oxygen atmosphere onto single crystalline Co_2TiO_4 (001), $Co_{1.75}Mn_{0.25}TiO_4$ (001), and $Co_{1.25}Fe_{0.5}Mn_{0.25}TiO_4$ (001) substrates. These substrates were annealed for two hours at 400 $^{\circ}\mathrm{C}$ in an oxygen pressure of 3×10^{-7} mbar to obtain a clean and well-ordered surface structure prior to the Fe_3O_4 deposition. The substrate temperature was kept at 250 $^{\circ}\mathrm{C}$ in an oxygen pressure of 1×10^{-6} mbar during growth. The Fe flux was calibrated using a quartz-crystal monitor at the growth position prior to deposition and set to 1 Å per minute for the growth of all films. *In situ* and *real-time* monitoring of the epitaxial growth was performed by reflection high-energy electron diffraction (RHEED) measurements, which were taken at 20 keV electron energy, with the beam aligned parallel to the [100] direction of the substrate. The crystalline structure was also verified *in situ* after the growth by low-energy electron diffraction (LEED), which was recorded at the electron energy of 88 eV. All samples were analyzed *in situ* by x-ray photoelectron spectroscopy (XPS). The XPS data were collected using 1486.6 eV photons

(monochromatized Al K_α light) in a normal emission geometry and at room temperature using a Scienta R3000 electron energy analyzer. The overall energy resolution was set to be about 0.3 eV. X-ray diffraction (XRD) was employed for further *ex situ* investigation of the structural quality and the microstructure of the films. The XRD measurements were performed with a high resolution Philips X'Pert MRD diffractometer using monochromatic Cu $K_{\alpha 1}$ radiation (λ = 1.54056 Å). Temperature dependent resistivity (ρ) measurements of the Fe_3O_4 thin films were performed by the standard four probe technique using a Physical Property Measurement System (PPMS). The ρ-*T* curves for all the samples were measured with a current source of 0.1 μA from 300 to 80 K and back to 300 K at zero field.

Acknowledgments

The authors acknowledge valuable comments from S. Wirth. The research of X. H. L. was supported by the Max Planck-POSTECH Center for Complex Phase Materials.

Competing financial interests

The authors declare no competing financial interests.

Author contributions

X. H. L. grew and characterized the films with the help from C. F. C. and A. D. R.. X. H. L. carried out the electrical transport and magnetic properties measurements. A. C. K. grew and characterized the substrates. X. H. L., C. F. C. and L. H. T. performed the data analysis and wrote the manuscript.

References

[1] de Groot, R. A., Müller, F. M., van Engen, P. G. & Buschow, K. H. J. New Class of Materials: Half-Metallic Ferromagnets. *Phys. Rev. Lett.* **50**, 2024-2027 (1983).

[2] Yanase, A. & Siratori, K. Band Structure in the High Temperature Phase of Fe_3O_4. *J. Phys. Soc. Jpn.* **53**, 312-317 (1984).

[3] Li, X. W., Gupta, A., Xiao, G., Qian, W. & Dravid, V. P. Fabrication and properties of heteroepitaxial magnetite (Fe_3O_4) tunnel junctions. *Appl. Phys. Lett* **73**, 3282 (1998).

[4] Greullet, F., Snoeck, E., Tiusan, C., Hehn, M., Lacour, D., Lenoble, O., Magen, C. & Calmels, L. Large inverse magnetoresistance in fully epitaxial Fe/Fe_3O_4/MgO/Co magnetic tunnel junctions. *Appl. Phys. Lett* **92**, 053508 (2008).

[5] Chambers, S. A. Epitaxial growth and properties of thin film oxides. *Surf. Sci. Rep.* **39**, 105-180 (2000).

[6] Ziese, M. Extrinsic magnetotransport phenomena in ferromagnetic oxides. *Rep. Prog. Phys.* **65** 143-249 (2002).

[7] Moussy, J. B. From epitaxial growth of ferrite thin films to spin-polarized tunnelling. *J. Phys. D: Appl. Phys.* **46** 143001(1-27) (2013).

[8] Mijiritskii, A. V. & Boerma, D. O. The (001) surface and morphology of thin Fe_3O_4 layers grown by O_2-assisted molecular beam epitaxy. *Surf. Sci.* **486**, 73-81 (2001).

[9] Verwey, E. J. W. Electronic Conduction of Magnetite (Fe_3O_4) and its Transition Point at Low Temperatures. *Nature* **144**, 327-328 (1939).

[10] Gong, G. Q., Gupta, A., Xiao, G., Qian, W. & Dravid, V. P. Magnetoresistance and magnetic properties of epitaxial magnetite thin films. *Phys. Rev. B* **56**, 5096 (1997).

[11] Eerenstein, W., Palstra, T. T. M., Hibma, T. & Celotto, S. Origin of the increased resistivity in epitaxial Fe_3O_4 films. *Phys. Rev. B* **66**, 201101(R) (2002).

[12] Arora, S. K., Sofin, R. G. S. & Shvets, I. V. Magnetoresistance enhancement in epitaxial magnetite films grown on vicinal substrates. *Phys. Rev. B* **72**, 134404 (2005).

[13] Geprags, S., Mannix, D., Opel, M., Goennenwein, S. T. B. & Gross. R. Converse magnetoelectric effects in Fe_3O_4/$BaTiO_3$ multiferroic hybrids. *Phys. Rev. B* **88**, 054412 (2013).

[14] Aragon, R., Gehring, P. M. & Shapiro, S. M. Stoichiometry, percolation, and Verwey ordering in magnetite. *Phys. Rev. Lett* **70**, 1635 (1993).

[15] Brabers, V. A. M., Walz, F. & Kronmüller, H. Impurity effects upon the Verwey transition in magnetite. *Phys. Rev. B* **58**, 14163 (1998).

[16] Liu, X. H., Rata, A. D., Chang, C. F., Komarek, A. C. & Tjeng, L. H. Verwey transition in Fe_3O_4 thin films: Influence of oxygen stoichiometry and substrate-induced microstructure. *Phys. Rev. B* **90**, 125142 (2014).

[17] Imada, M., Fujimori, A. & Tokura, Y. Metal-insulator transitions. *Rev. Mod. Phys.* **70** 1039 (1998).

[18] Brockman, J. Samant, M. G. Roche, K. P. & Parkin, S. S. P. Substrate-induced disorder in V_2O_3 thin films grown on annealed c-plane sapphire substrates. *Appl. Phys. Lett.* **101**, 051606 (2012).

[19] Sakai, J., Limelette, P. & Funakubo, H. Transport properties and c/a ratio of V_2O_3 thin films grown on C- and R-plane sapphire substrates by pulsed laser deposition. *Appl. Phys. Lett.* **107**, 241901 (2015).

[20] Hepting, M., Minola, M., Frano, A., Cristiani, G., Logvenov, G., Schierle, E., Wu, M., Bluschke, M., Weschke, E., Habermeier, H. U., Benckiser, E., Tacon, M. L. & Keimer, B.

Tunable Charge and Spin Order in $PrNiO_3$ Thin Films and Superlattices. *Phys. Rev. Lett.* **113**, 227206 (2014).

[21] Mikheev, E., Hauser, A. J., Himmetoglu, B., Moreno, N. E., Janotti, A., Van de Walle, C. G. & Stemmer, S. Tuning bad metal and non-Fermi liquid behavior in a Mott material: Rare-earth nickelate thin films. *Sci. Adv.* **1**, 1500797(1-7) (2015).

[22] Zhang, J. Y., Kim, H., Mikheev, E., Hauser, A. J. & Stemmer, S. Key role of lattice symmetry in the metal-insulator transition of $NdNiO_3$ films. *Sci. Rep.* **6**, 23652(1-7) (2016).

[23] Shi, J., Ha, S. D., Zhou, Y., Schoofs, F. & Ramanathan, S. A correlated nickelate synaptic transistor. *Nat. Commun.* **4**, 2676(1-9) (2013).

[24] Nakagiri, N., Manghnani, M. H., Ming, L. C. & Kimura, S. Crystal structure of magnetite under pressure. *Phys. Chem. Minerals* **13**, 238-244 (1986).

[25] Ramasesha, S. K., Mohan, M., Singh, A. K., Honig, J. M. & Rao, C. N. R. High-pressure study of Fe_3O_4 through the Verwey transition. *Phys. Rev. B* **50**, 13789 (1994).

[26] Rozenberg, G. K., Hearne, G. R., Pasternak, M. P., Metcalf, P. A. & Honig, J. M. Nature of the Verwey transition in magnetite (Fe_3O_4) to pressures of 16 GPa. *Phys. Rev. B* **53**, 6482 (1996).

[27] Brabers, J. H. V. J., Walz, F. & Kronmüller, H. The role of volume effects in the Verwey transition in magnetite. *J. Phys.: Condens. Matter* **11**, 3679-3686 (1999).

[28] Mott, N. F. Electrons in disordered structures. *Adv. Phys.* **16**, 49-144 (1967).

[29] Cullen, J. R. & Callen, E. R. Multiple Ordering in Magnetite. *Phys. Rev. B* **7**, 397 (1973).

[30] Wright, J. P., Attfield, J. P. & Radaelli, P. G. Long Range Charge Ordering in Magnetite Below the Verwey Transition. *Phys. Rev. Lett.* **87**, 266401 (2001).

[31] Senn, M. S., Wright, J. P. & Attfield, J. P. Charge order and three-site distortions in the Verwey structure of magnetite. *Nature* **481**, 173-176 (2012).

[32] Tanaka, A., Chang, C. F., Buchholz, M., Trabant, C., Schierle, E., Schlappa, J., Schmitz, D., Ott, H., Metcalf, P., Tjeng, L. H. & Schüßler-Langeheine, C. Analysis of charge and orbital order in Fe_3O_4 by Fe $L_{2,3}$ resonant x-ray diffraction. *Phys. Rev. B* **88**, 195110 (2013).

Figure legends

Figure 1. RHEED and LEED images. Representative RHEED patterns of clean **a**, MgO (001), **b**, Co_2TiO_4 (001), **c**, $Co_{1.75}Mn_{0.25}TiO_4$ (001), and **d**, $Co_{1.25}Fe_{0.5}Mn_{0.25}TiO_4$ (001) substrates. RHEED and LEED patterns, respectively, of 40 nm Fe_3O_4 films grown on MgO (001) **e** and **i**, on Co_2TiO_4 (001) **f** and **j**, on $Co_{1.75}Mn_{0.25}TiO_4$ (001) **g** and **k**, and on $Co_{1.25}Fe_{0.5}Mn_{0.25}TiO_4$ (001) **h** and **l**.

Figure 2. Electrical transport properties. **a**, Resistivity as a function of temperature of 40 nm Fe_3O_4 thin films grown on MgO (001), Co_2TiO_4 (001), $Co_{1.75}Mn_{0.25}TiO_4$ (001), and $Co_{1.25}Fe_{0.5}Mn_{0.25}TiO_4$ (001) substrates and of single crystal bulk Fe_3O_4. **b**, The Verwey transition temperature (T_{V+}) as a function of film thickness of the films grown on MgO (001), Co_2TiO_4 (001), $Co_{1.75}Mn_{0.25}TiO_4$ (001), and $Co_{1.25}Fe_{0.5}Mn_{0.25}TiO_4$ (001) substrates, the black horizontal line represents the T_{V+} of a stoichiometric bulk magnetite crystal.

Figure 3. Reciprocal space maps. Reciprocal space mapping of the (1 1 5)-reflection of **a**, a 200 nm Fe_3O_4 film grown on Co_2TiO_4 (001), and of **b**, a 80 nm Fe_3O_4 film grown on $Co_{1.25}Fe_{0.5}Mn_{0.25}TiO_4$ (001).

Table1. Lattice constants. Lattice constants of 40 nm, 80 nm, and 200 nm Fe_3O_4 thin films on Co_2TiO_4, $Co_{1.75}Mn_{0.25}TiO_4$, and $Co_{1.25}Fe_{0.5}Mn_{0.25}TiO_4$.

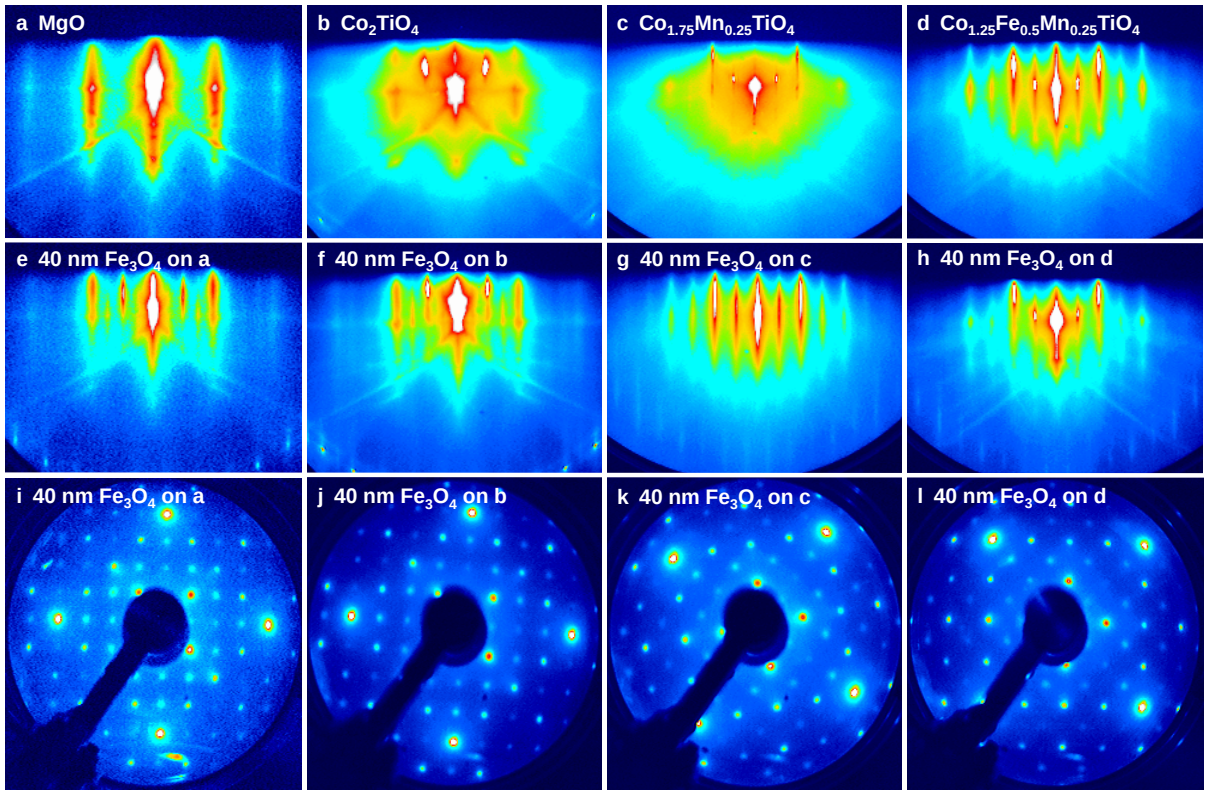

Figure 1:

	Substrate a	40 nm Fe_3O_4 c	80 nm Fe_3O_4 c	200 nm Fe_3O_4 c
Co_2TiO_4	8.4528 Å	8.3332 Å	8.3330 Å	8.3316 Å
$Co_{1.75}Mn_{0.25}TiO_4$	8.4797 Å	8.3042 Å	8.3048 Å	8.3054 Å
$Co_{1.25}Fe_{0.5}Mn_{0.25}TiO_4$	8.4898 Å	8.2800 Å	8.2806 Å	8.2855 Å

Table 1:

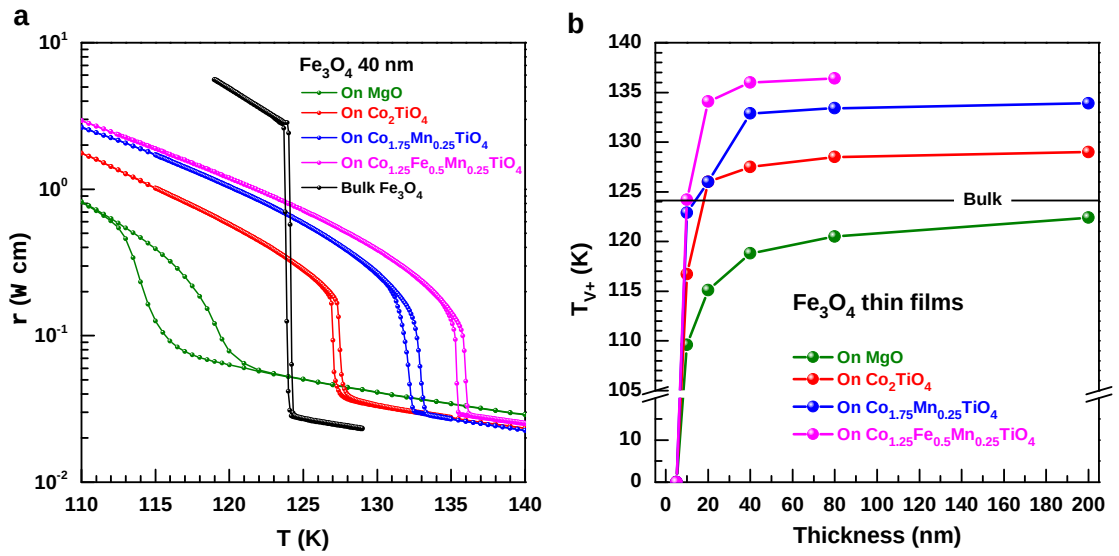

Figure 2:

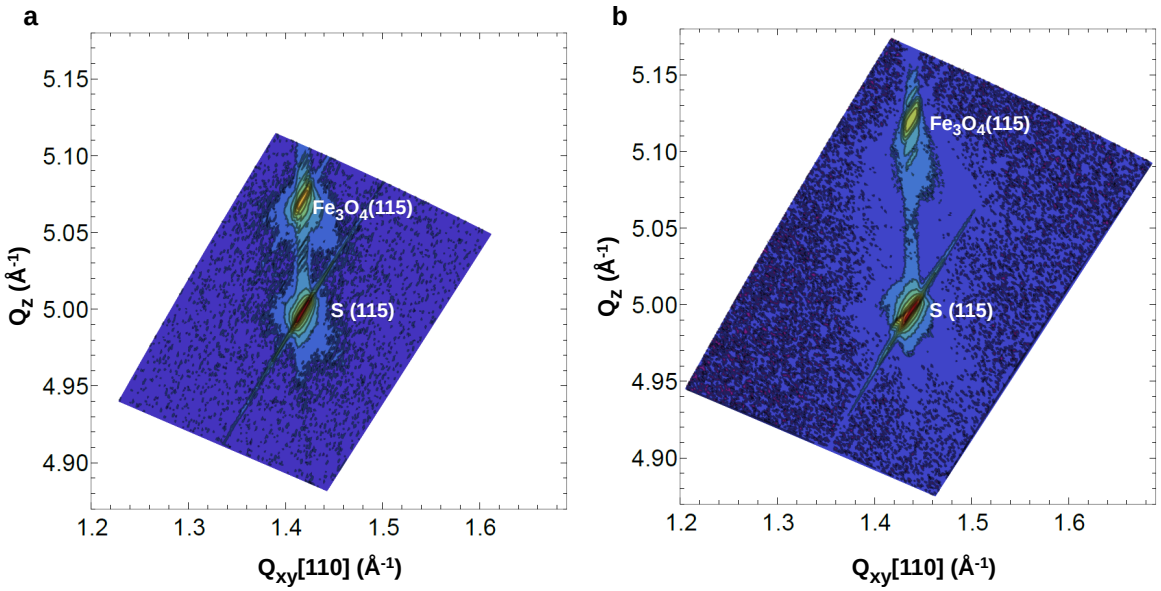

Figure 3:

Supplementary Information

Substrates Characterization We confirmed the sample quality of our Co_2TiO_4 single crystals by powder X-ray diffraction, Laue diffraction and single crystal X-ray diffraction measurements as well as by complementary magnetization measurements. Co_2TiO_4 crystallizes in the cubic spinel structure AB_2O_4 with space group $Fd\bar{3}m$. From the powder X-ray diffraction measurements (Cu-K_α radiation) it is evident that there appears to be no impurity phase within our Co_2TiO_4 crystals, see Fig. S1. The lattice parameter a of the cubic unit cell amounts to a=8.45276(20) Å. Laue as well as single crystal X-ray diffraction measurements confirm the single crystallinity of our crystals, see Fig. S2a. The crystal structure of a spherical Co_2TiO_4 sample has been measured by means of single crystal X-ray diffraction on a Bruker D8 VENTURE X-ray diffractometer (equipped with a bent monochromator, CMOS large area detector and a Mo-K_α X-ray tube). 4280 reflections have been measured up to $2\Theta_{max} = 135.1°$ with a redundancy of 14.76. The internal R-value of the data collection amounts to 2.37%. The only free structural parameter apart from the atomic displacement parameters is the x-position of the oxygen ion which amounts to x(O1)=0.26019(6). The displacement parameters amount to U_{iso}(Co1)=0.00641(2) Å^2, U_{iso}(Ti1/Co2)=0.006450(2) Å^2, U_{iso}(O1)=0.01131(5) Å^2 which are reasonably small. Finally, the refinement of the *A*-site and *B*-site occupancies indicates that the tetrahedral *A*-site is solely occupied by the Co^{2+}-ions, whereas roughly a 50%:50% statistical distribution of Ti^{4+} and Co^{2+}-ions is observed at the octahedral *B*-sites, i.e. the refined *A*-site Co^{2+} occupancy amounts to 99.53(1)%, see Fig. S2b. The goodness of the fit of this structural refinement on F^2 amounts to GoF=1.81, and the R- and weighted R-values amount to R=1.77% and Rw=4.79% respectively, thus, indicating a high reliability of our crystal structure determination. A complementary magnetization measurement of Co_2TiO_4 on a SQUID magnetometer (0.1 T field- and zero-field-cooled measurements) indicates a magnetic ordering temperature around 50 K with a behavior that is very similar as described in literature, [1] just that the ferrimagnetic ordering temperature appears to be distinctly higher (and with sharper transition) in our crystals, thus, indicating the high crystal quality of our Co_2TiO_4 single crystals, see Fig. S3.

In order to change the strain exerted by the substrate we have doped Mn and Fe into the Co_2TiO_4 matrix. In Fig. S1 the results of our Rietveld fits are shown also for these $Co_{2-x-y}Fe_yMn_xTiO_4$ systems and indicate that there are no detectable impurity phases in our single crystals. The lattice parameters amount to a=8.45276(20) Å, 8.47974(26) Å and 8.48980(28) Å for Co_2TiO_4, $Co_{1.75}Mn_{0.25}TiO_4$ and $Co_{1.25}Fe_{0.5}Mn_{0.25}TiO_4$ respectively. Laue diffraction and single crystal X-ray diffraction measurements were also done on the co-doped $Co_{2-x-y}Fe_yMn_xTiO_4$ single crystals and prove the single crystallinity of all our samples.

References

[1] J. Hubsch and G. Gavoille. Semi-spin-glass behavior in the Co_2TiO_4 compound. *Phys. Rev. B* **26**, 3815 (1982).

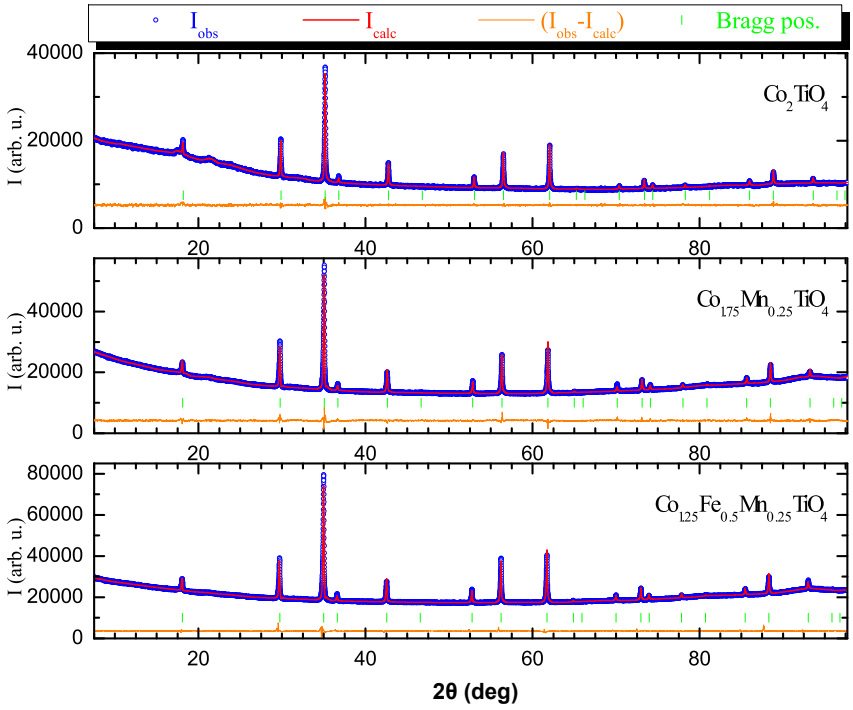

Figure S1. Rietveld refinement results of powder X-ray diffraction measurements of our $Co_{2-x-y}Fe_yMn_xTiO_4$ crystals (obtained from single crystals crushed to powder). As indicated by the difference line (Iobs-Icalc), there are no impurity phases in our single crystals. Some minor background problems are artificial observations within our powder X-ray diffraction measurements originating from the measurement configuration and not intrinsically from our sample (around 20° - 25° in 2Θ). The lattice parameters amount to a= 8.45276(20) Å, 8.47974(26) Å, and 8.48980(28) Åfor Co_2TiO_4, $Co_{1.75}Mn_{0.25}TiO_4$, and $Co_{1.25}Fe_{0.5}Mn_{0.25}TiO_4$ respectively.

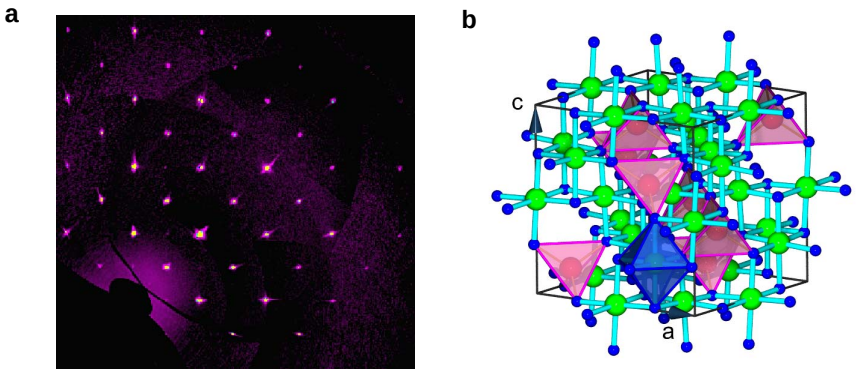

Figure S2. **a**, X-ray scattering intensities of Co_2TiO_4 within the HK0 plane of reciprocal space. Obviously, our sample is a single phase single crystal without any other crystallites. **b**, Visualization of the crystal structure derived from our single crystal X-ray diffraction measurements of Co_2TiO_4. Red/blue spheres: Co-/O-ions; green spheres: 50% Co-ions and 50% Ti-ions.

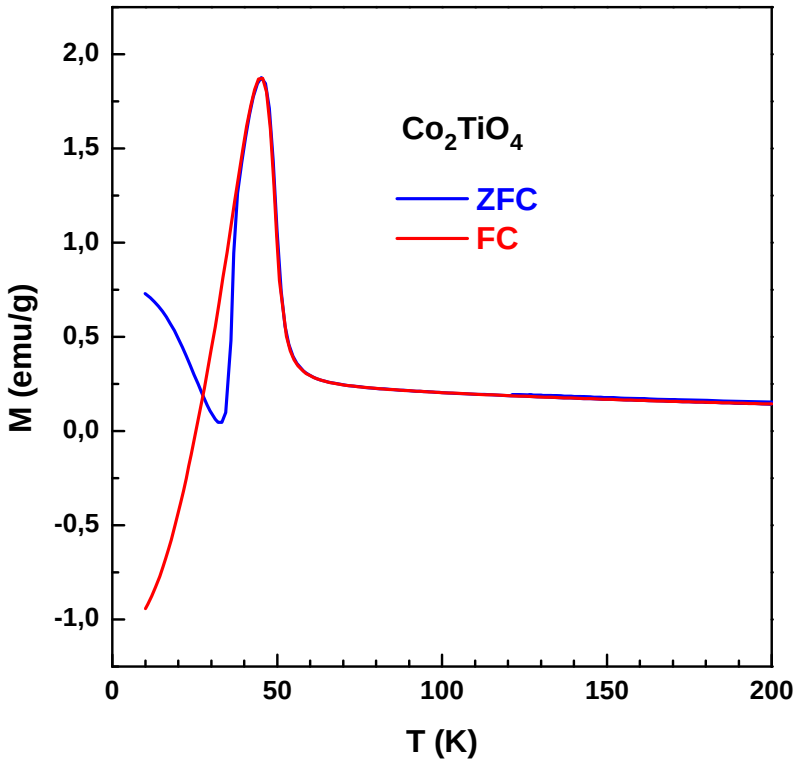

Figure S3. Magnetic susceptibility measurements of Co_2TiO_4 with an applied magnetic field of 0.1 T, confirming not only the high crystal quality indicated by the sharp magnetic transition at comparably high transition temperature, but also indicate there is no magnetic transition from the substrate in the interesting temperature regime around the Verwey transition.

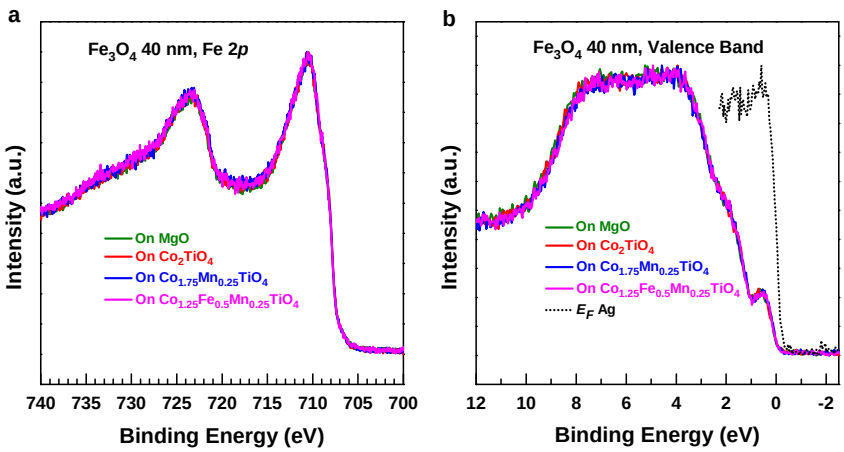

Figure S4. **a**, XPS Fe $2p$ core-level spectra, and **b**, valence band spectra of 40 nm Fe_3O_4 films on MgO, Co_2TiO_4, $Co_{1.75}Mn_{0.25}TiO_4$, and $Co_{1.25}Fe_{0.5}Mn_{0.25}TiO_4$.